# South Pole neutron monitor forecasting of solar proton radiation intensity

S. Y. Oh,[1,2] J. W. Bieber,[2] J. Clem,[2] P. Evenson,[2] R. Pyle,[2] Y. Yi,[1] and Y.-K. Kim[3]

Received 27 March 2012; accepted 4 April 2012; published 25 May 2012.

[1] We describe a practical system for forecasting peak intensity and fluence of solar energetic protons in the tens to hundreds of MeV energy range. The system could be useful for forecasting radiation hazard, because peak intensity and fluence are closely related to the medical physics quantities peak dose rate and total dose. The method uses a pair of ground-based detectors located at the South Pole to make a measurement of the solar particle energy spectrum at relativistic (GeV) energies, and it then extrapolates this spectrum downward in energy to make a prediction of the peak intensity and fluence at lower energies. A validation study based upon 12 large solar particle events compared the prediction with measurements made aboard GOES spacecraft. This study shows that useful predictions (logarithmic correlation greater than 50%) can be made down to energies of 40–80 MeV (GOES channel P5) in the case of peak intensity, with the prediction leading the observation by 166 min on average. For higher energy GOES channels, the lead times are shorter, but the correlation coefficients are larger.

**Citation:** Oh, S. Y., J. W. Bieber, J. Clem, P. Evenson, R. Pyle, Y. Yi, and Y.-K. Kim (2012), South Pole neutron monitor forecasting of solar proton radiation intensity, *Space Weather*, *10*, S05004, doi:10.1029/2012SW000795.

## 1. Introduction

[2] Radiation exposure is one of the most intractable problems of space flight, both in terms of human health and in terms of damage to sensitive electronic systems. Radiation from Galactic cosmic rays is continuously present and must be factored into mission planning, especially for long-term flight in deep space.

[3] Radiation from solar cosmic rays, in contrast, is episodic and highly variable, but also highly dangerous. In interplanetary space, an unprepared astronaut could suffer severe injury from radiation exposure during a major solar particle event [*Hu et al.*, 2009].

[4] The most extreme solar particle events have sufficient energy and intensity to raise radiation levels within Earth's atmosphere and on Earth's surface. These events, termed Ground Level Enhancements (GLE), are of concern for pilots and air crews [*Lantos*, 2005], especially for those flying polar routes where shielding from Earth's magnetic field is negligible.

[5] Owing to velocity dispersion, the GLE particles, traveling near the speed of light, arrive sooner and reach a peak more quickly than the lower energy particles. This work shows that the energy spectrum in the GLE energy range can be used to make useful predictions of peak intensity and fluence (as a function of energy) of the later-arriving, lower-energy particles measured by GOES spacecraft. This is significant for space weather forecasting of radiation hazard, because peak intensity and fluence are, respectively, the physical quantities that determine peak radiation dose rate and total radiation dose.

## 2. Data and Method

[6] For many years there were two types of neutron monitor at the South Pole: a standard 3NM64 and a set of "bare" (without the lead producer but enclosed in polyethylene moderators) BP-28 detectors. These "Polar Bares" had a lower total counting rate, but were relatively more sensitive to solar cosmic rays than the standard NM64. Both sets of detectors were at mountain altitude (2820 m) with a rigidity threshold (governed by atmospheric absorption) of approximately 1 GV. Relative count rates (% increase) of the 12 GLEs in our study are shown in Figures 1 and 2 as recorded by the standard neutron monitor (3NM64) and the set of Polar Bare (PB) detectors. All data are 2-min or 5-min averages corrected to standard pressure (760 mm Hg) using an assumed solar particle absorption length of 100 g cm$^{-2}$ [*Duggal*, 1979]. Count rates are expressed as a percent increase over the pre-event Galactic background. In the figures we give the actual dates

[1]Department of Astronomy and Space Science, Chungnam National University, Daejeon, South Korea.
[2]Bartol Research Institute, Department of Physics and Astronomy, University of Delaware, Newark, Delaware, USA.
[3]Department of Nuclear Engineering, Hanyang University, Seoul, South Korea.

Corresponding author: S. Y. Oh, Department of Astronomy and Space Science, Chungnam National University, Daejeon, 305-764, South Korea. (osy1999@cnu.ac.kr)

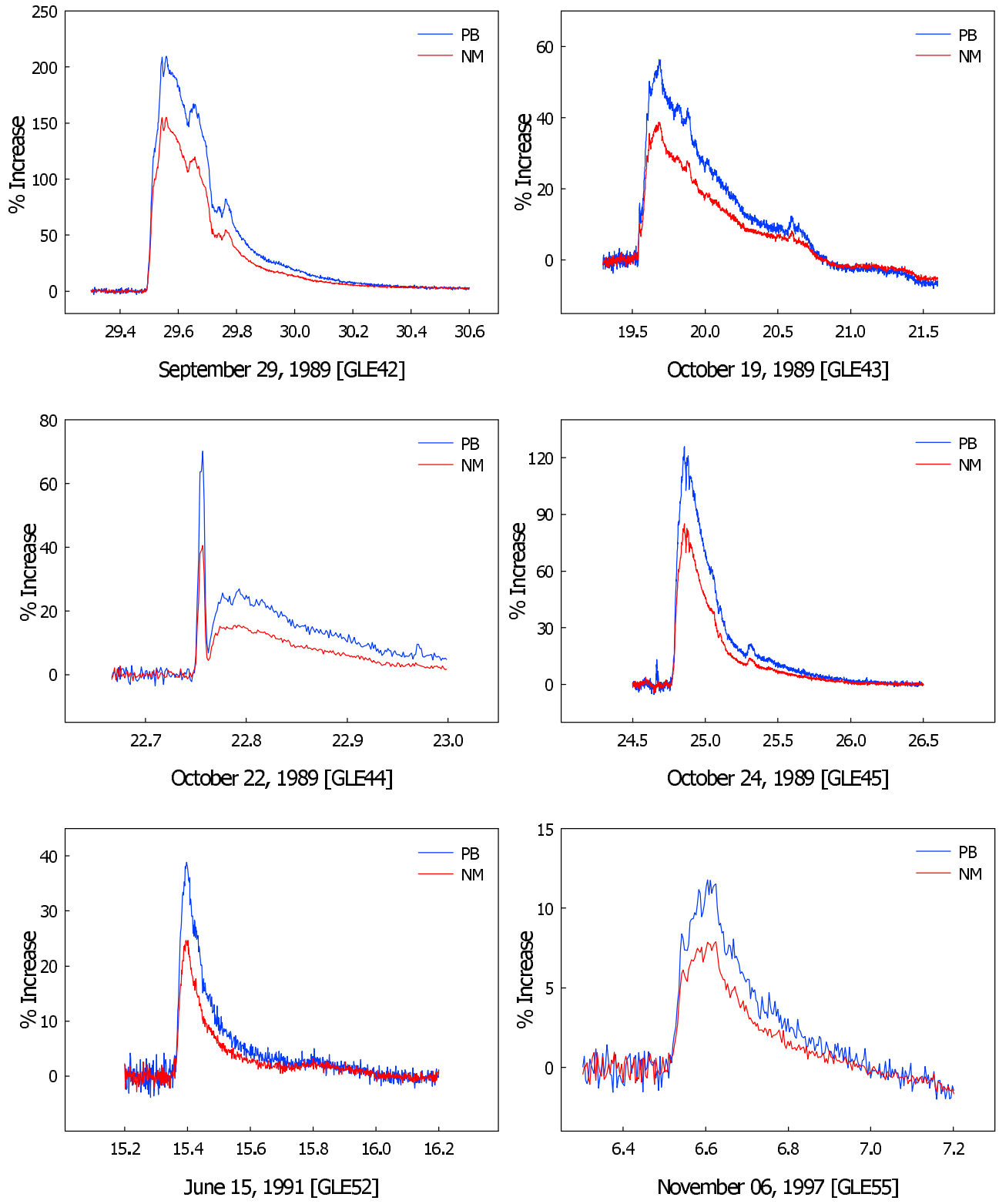


**Figure 1.** Relative count rates (% increase) of 6 GLEs recorded by a standard neutron monitor (NM) and by "Polar Bare" (PB) neutron detectors.

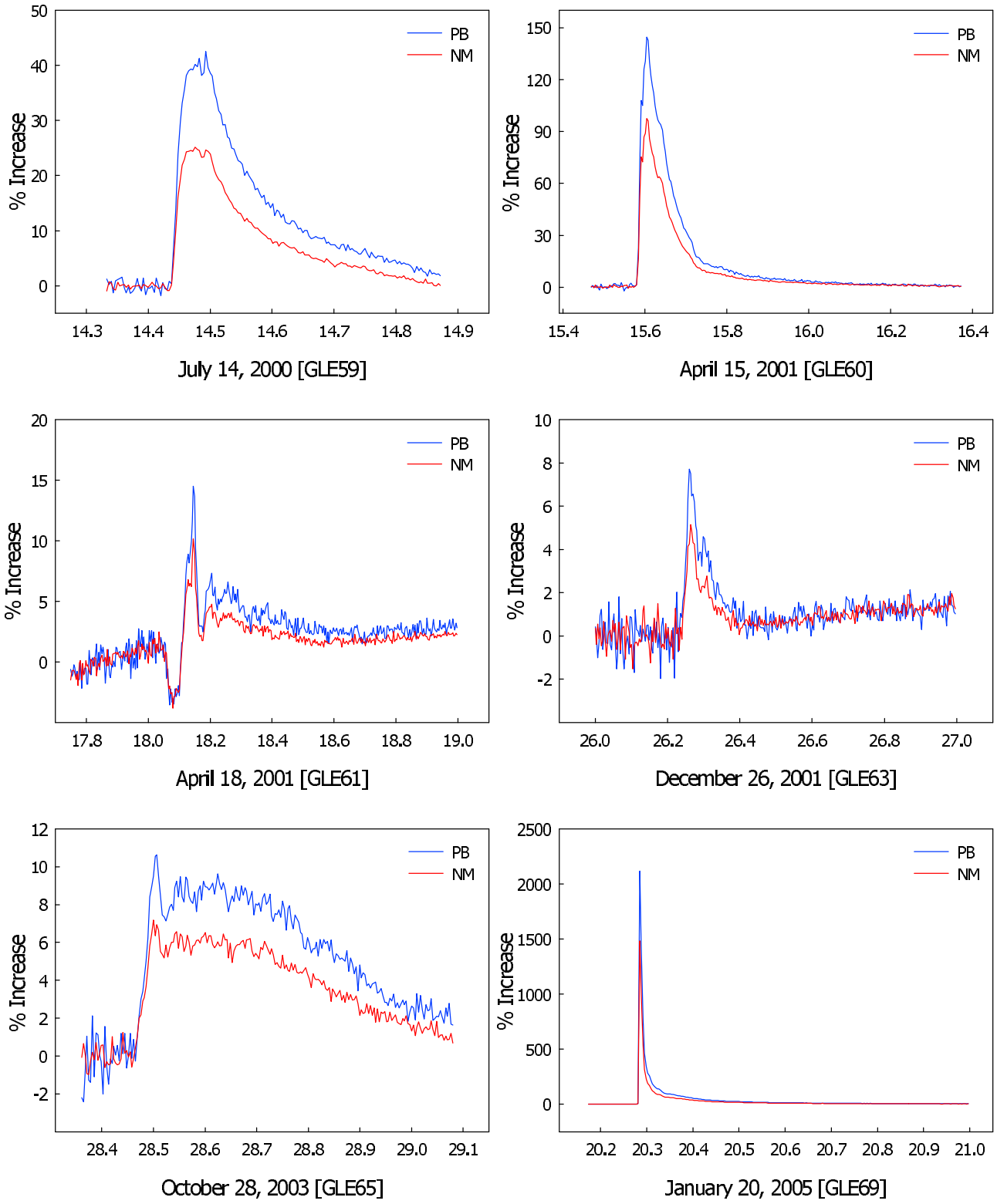


**Figure 2.** Count rates, as in Figure 1, for 6 additional GLEs.

**Table 1.** List of 12 GLEs Including Parameters of the Energy Spectrum at Peak[a]

| Event | Date | Peak Time | PB (%) | NM (%) | $j_0$ | $j_{e0}$ | $\gamma$ |
|---|---|---|---|---|---|---|---|
| GLE42 | 29 Sep 1989 | 13:04 | 208.7 | 154.8 | 2.0E+01 | 2.7E-02 | 4.0 |
| GLE43 | 19 Oct 1989 | 15:50 | 53.0 | 35.9 | 1.0E+01 | 1.4E-02 | 4.8 |
| GLE44 | 22 Oct 1989 | 18:05 | 58.3 | 35.7 | 1.9E+01 | 2.6E-02 | 6.2 |
| GLE45 | 24 Oct 1989 | 20:34 | 125.7 | 85.0 | 2.4E+01 | 3.3E-02 | 4.9 |
| GLE52 | 15 Jun 1991 | 09:32 | 38.8 | 24.4 | 1.2E+01 | 1.6E-02 | 5.8 |
| GLE55 | 06 Nov 1997 | 14:30 | 11.8 | 7.9 | 2.5E+00 | 3.4E-03 | 5.0 |
| GLE59 | 14 Jul 2000 | 11:25 | 40.2 | 25.1 | 1.2E+01 | 1.7E-02 | 5.9 |
| GLE60 | 15 Apr 2001 | 14:30 | 144.6 | 97.6 | 2.8E+01 | 3.9E-02 | 4.9 |
| GLE61 | 18 Apr 2001 | 03:30 | 14.5 | 10.2 | 2.2E+00 | 3.0E-03 | 4.5 |
| GLE63 | 26 Dec 2001 | 06:20 | 7.5 | 5.1 | 1.3E+00 | 1.8E-03 | 4.7 |
| GLE65 | 28 Oct 2003 | 12:10 | 10.6 | 6.9 | 2.5E+00 | 3.5E-03 | 5.2 |
| GLE69 | 20 Jan 2005 | 06:50 | 2116.6 | 1483.6 | 3.2E+02 | 4.4E-01 | 4.5 |

[a] $\gamma$: rigidity spectral index; $j_0$: $j = j_0 \times P^{-\gamma}$ [cm$^2$ s ster GV]$^{-1}$; $j_{e0}$: $j = j_{e0} \times P^{-\gamma}$ [cm$^2$ s ster MeV]$^{-1}$.

of the events, plus the generally recognized "GLE number" of the event. For brevity we often refer to the events by number in our discussion.

[7] The spectrum of relativistic solar protons can be estimated from the count rates as discussed by *Bieber and Evenson* [1991]. Briefly, with the aid of yield functions provided by *Stoker* [1985], the ratio PB/NM64 can be translated into a spectral index. Specifically we assume a spectrum in the form of a power law in rigidity ($P^{-\gamma}$, with $P$ the rigidity and $\gamma$ the spectral index) with an upper cutoff of 20 GV. Finally, with spectral shape known, the actual count rate can be used to determine the absolute spectrum amplitude.

[8] Two sets of constants for the Dorman function were suggested by *Stoker* [1985], which were designated "PB(1)" and "PB(2)" by *Bieber and Evenson* [1991]. However, *Bieber and Evenson* [1991] found that PB(2) provided better agreement with spectra derived by the traditional method of comparing observations made at different geomagnetic cutoffs. Therefore, we choose to base the current analysis on PB(2), for which the Dorman constants in the conventional notation are $\alpha = 7.846$ and $K = 0.940$.

[9] Table 1 summarizes the analysis of the 12 GLEs, giving both the input data at the time of peak intensity and the derived spectra at that time. Each spectrum is expressed in two different parameterizations, both of which have the same rigidity spectral index $\gamma$. With the parameter $j_0$ the spectrum is expressed as $j = j_0 \times P^{-\gamma}$ with units [cm$^2$ s ster GV]$^{-1}$. With the parameter $j_{e0}$ the spectrum is expressed as $j = j_{e0} \times P^{-\gamma}$ with the units being [cm$^2$ s ster MeV]$^{-1}$. The derived spectral index is often near 5, which was found to be quite typical of GLEs by *Duggal* [1979]. Some researchers find that GLEs are generally of the "gradual" type of solar particle event [*Reames*, 2009], while others argue that the impulsive-gradual classification is often misused [*Cliver and Cane*, 2002]. We will not delve into this issue here, because the distinction is not essential for our analysis.

[10] Because these are large events with small statistical errors, the uncertainties in the derived parameters $j_0$, $j_{e0}$, and $\gamma$ will generally be determined by systematic uncertainties, the most important of which is likely to be uncertainties in the specific yield function of the polar bares. As noted above, *Stoker* [1985] reported two limiting cases of Dorman function parameters that were both consistent with the latitude survey results. To gain an impression of the systematic uncertainties, we compared the Dorman function employed here, designated PB(2), with the other function, PB(1). For the spectrum amplitudes $j_0$ and $j_{e0}$, PB(2) yielded a result approximately a factor of two larger than PB(1). For $\gamma$, PB(2) yielded an index larger than PB(1), corresponding to a softer spectrum. The difference ranged from approximately 0.5 when $\gamma = 4.0$ to 1.9 when $\gamma = 6.2$. These differences may exaggerate the true systematic uncertainty, however, considering that PB(2) appears to provide better agreement with other methods of spectrum determination.

[11] GOES data were downloaded from the National Geophysical Data Center (NGDC, http://goes.ngdc.noaa.gov/data/avg/). We employ 5-min averages of the differential proton channels P4 to P10. Specifically, data of GOES 7 are used for GLEs 42–52, data of GOES 8 for GLE 55, data of GOES 10 for GLEs 59–65, and data of GOES 11 for GLE 69.

[12] Spectra derived from the PB/NM64 combination are displayed graphically in Figures 3 and 4 as dashed lines. GOES peak flux data from the same event are shown as solid circles. The open diamonds indicate points on the neutron monitor spectrum that are at the same energy as corresponding GOES channels. Energy ranges and mean energy of the various GOES channels are presented in Table 2. The first numbers in the energy range and mean energy columns apply to GOES 8 and higher numbered GOES satellites, while the numbers in parentheses apply to GOES 7 using the corrected energy ranges derived by *Smart and Shea* [1999]. Mean energy was defined in the conventional way, i.e., $\int Ej(E)\mathrm{d}E / \int j(E)\mathrm{d}E$, where $E$ is energy, $j(E)$ is the differential spectrum, and the range of integration extends from the lower to upper limit of the GOES channel. Here, we assumed a nominal spectrum $j(E) \propto E^{-2.5}$.

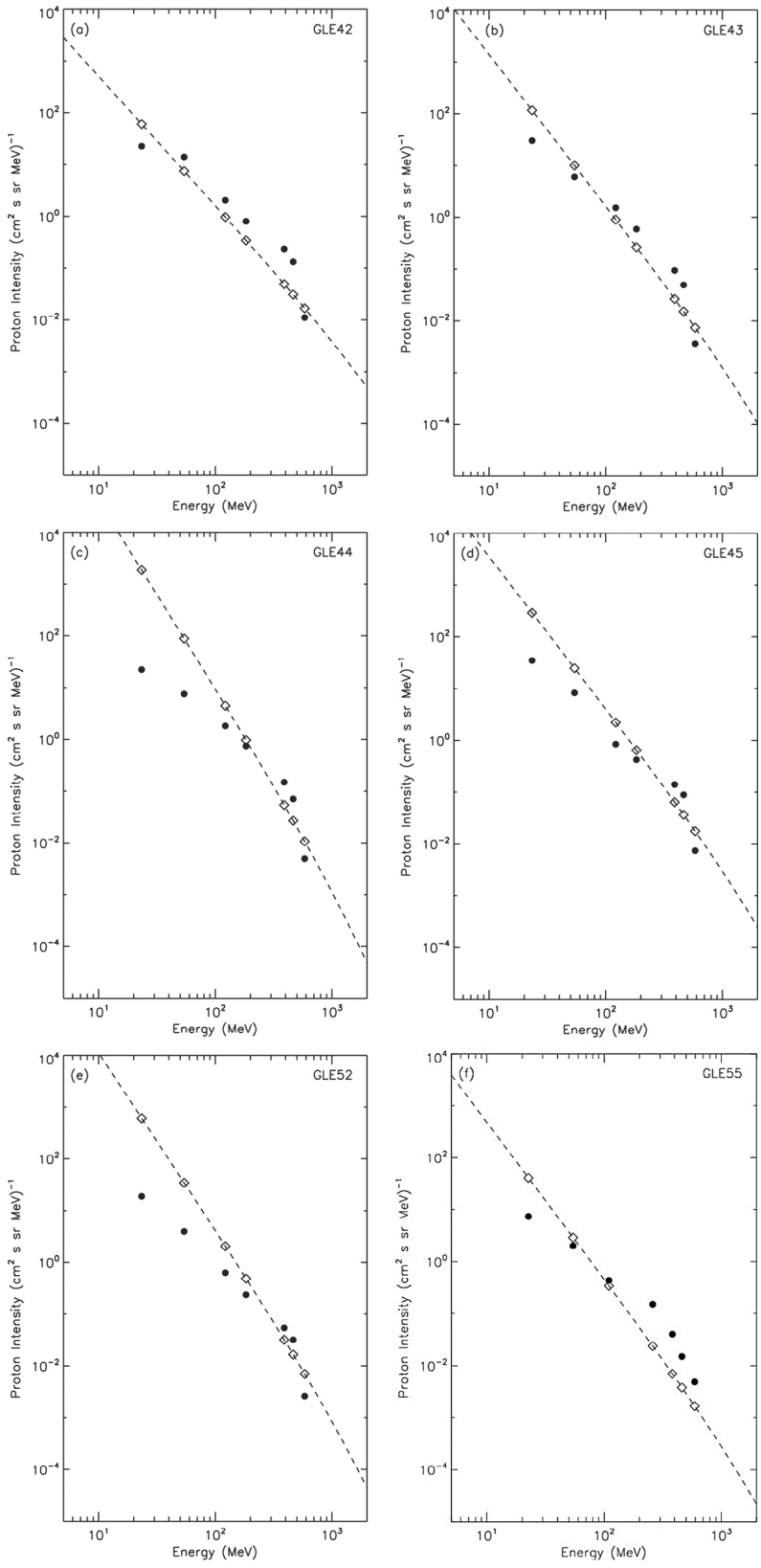
(a)
GLE42
(b)
GLE43
(c)
GLE44
(d)
GLE45
(e)
GLE52
(f)
GLE55
Proton Intensity (cm² s sr MeV)⁻¹
Energy (MeV)

**Figure 3**

[13] Since the spectra shown are all peak flux spectra, the neutron monitor spectra are always from a significantly earlier time. Hence we refer to the fluxes indicated by diamonds as our "prediction" of the subsequent GOES flux.

## 3. Results

[14] Figure 5 compares peak intensities measured for the P4–P10 proton energy channels as observed by GOES and predicted (as discussed above) from South Pole GLE spectra (In the case of GOES events with multiple peaks, we used the first peak.). As the energy of the proton channel gets higher, the correlation of observed and predicted intensities clearly gets progressively better.

[15] Figure 6 is similar to Figure 5, except the comparison is with the fluence from GOES. The fluence of each proton channel is time-integrated flux from onset to end of the event, determined as the time to return to the pre-event intensity level. The correlations displayed in Figure 6 could be used to define a relationship (via linear regression) between peak intensity predicted from the PB/NM64 combination and fluence measured in the corresponding GOES energy channel, thereby enabling predictions of fluence.

[16] We do not discuss the relation between fluence as measured at the South Pole and GOES because the fluence can only be determined when the event is over, and this paper concerns the predictive power of our system. For this reason we also note, but do not discuss further, that *Tylka and Dietrich* [2009] published integral fluence spectra for the 24 October 1989 event and 15 April 2001 event while *Usoskin et al.* [2009] published such spectra for the 20 January 2005 event. These correspond to Events 45, 60, and 69 in our Figures 3 and 4. Comparison of spectra obtained by the Polar Bare method with their results is an important objective of our future work.

[17] The relationships apparent in Figures 5 and 6 can be quantified by the correlation coefficients and residuals given in Table 2, both of which were computed from logarithmic representations of the data. Generally, we consider logarithmic correlation coefficients and residuals for these data to be more meaningful than linear ones, because intense solar particle events approximately obey a lognormal distribution in fluence [*Feynman et al.*, 1990] and peak intensity [*Pereyaslova et al.*, 1996]. Values based upon linear quantities tend to be dominated by the characteristics of one or two of the largest events in the dataset.

[18] The correlations listed in Table 2 confirm the visual impression in Figures 5 and 6 that the predictive power of spectra determined from South Pole data increases progressively with increasing GOES energy channel, and that the predictive power for peak intensity is better than that for fluence. Many of the correlations shown in Table 2 are significantly better than would be obtained by chance. For a sample of 12 events, a correlation greater than 50% has significance (one-tailed test) better than 0.95. For 60% correlations, the significance is better than 0.98, and for 70% correlations it is almost 0.995.

[19] Residuals and standard deviations in Table 2 likewise confirm the visual impressions from Figures 5 and 6. The mean residual of peak intensity is negative for the three lowest GOES channels, i.e., the GOES observation is less than the prediction from neutron monitors. This is probably a manifestation of a rollover in the low-energy spectrum [e.g., *Tylka and Dietrich*, 2009], which cannot be modeled by our assumption of a pure power law extending downward from neutron monitor energies. The standard deviations confirm both the visual impression of less scatter toward higher energies, and of less scatter in the predicted peak intensity than in the fluence when compared at the same energy. (We do not display mean residuals for fluence, because the units are different on the abscissa and ordinate of Figure 6. Hence, the results would depend on the units of time used.)

[20] We note that the peak of the GLE precedes the peak of the proton energy channel in most events. For instance, for the Bastille event (14 July 2000), the neutron monitor peak preceded the P4, P6, and P8 peaks by 320, 305, and 30 min respectively. As the energy of the proton energy channel gets higher, the time interval between the two peaks gets shorter. Typically the interval is less than 60 min for proton channels P8 and higher. Average time delays and standard deviations are summarized in Table 3.

[21] Finally, in Figure 7 we display these relationships for one event in the time domain. We show the percentage neutron monitor increase of GLE 69 (20 January 2005) and time profiles of GOES proton channel (P5, P6, P8) for the associated solar proton event.

## 4. Summary

[22] This work has demonstrated the feasibility of a practical system for forecasting peak intensity and fluence of solar energetic protons in the tens to hundreds of MeV energy range. If implemented, such a system could be useful for space weather forecasting of radiation hazard, because peak intensity and fluence are closely related to the medical physics quantities peak dose rate and total dose. Methods for converting the differential energy spectrum of a particular particle species into dose are available [*Wilson et al.*, 1989; *Schwadron et al.*, 2010], but implementing these methods is beyond the scope of the present

**Figure 3.** Peak-intensity energy spectra of 6 solar particle events. Dashed line indicates spectrum derived from neutron monitors at the time of the neutron monitor peak. Solid circles indicate peak proton flux from GOES plotted at the mean energy of the channel. Open diamonds indicate predicted proton intensity of the GOES channels, derived by extrapolating the neutron monitor spectrum downward in energy.

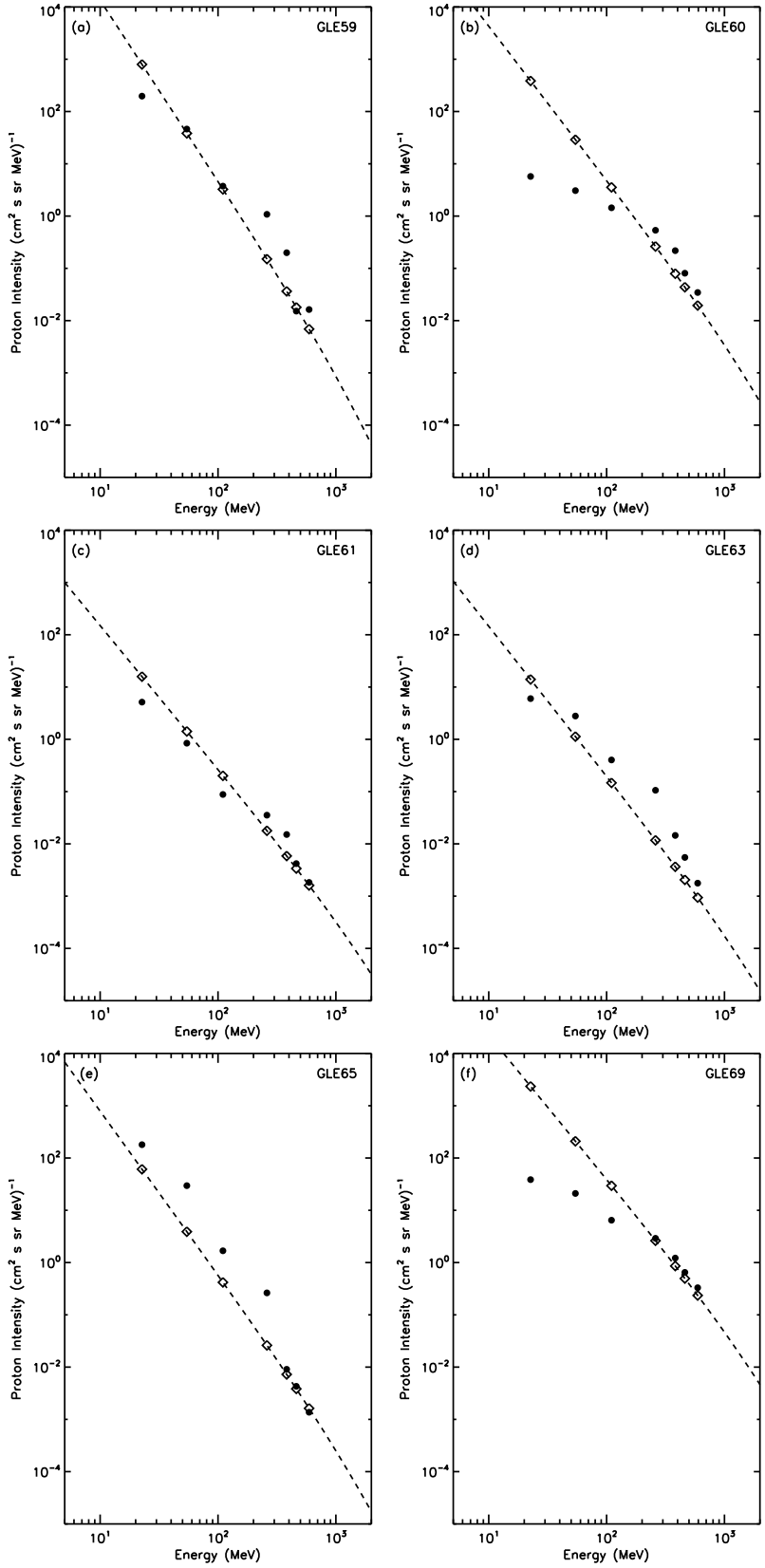


**Figure 4.** Peak-intensity energy spectra, as in Figure 3, but for 6 additional solar particle events.

**Table 2.** Correlation Coefficients and Residuals[a]

| Proton Channel | Energy Range of Channel (MeV) | Mean Energy of Channel (MeV) | Correlation Coefficients | | Mean Residual[b] (Standard Deviation[c]) | |
|---|---|---|---|---|---|---|
| | | | Peak Intensity | Fluence | Peak Intensity | Fluence |
| P4 | 15–40 (15–44) | 23 (23) | 0.41 | 0.36 | −0.89 (0.70) | (0.80) |
| P5 | 40–80 (39–82) | 54 (54) | 0.51 | 0.41 | −0.28 (0.60) | (0.73) |
| P6 | 80–165 (84–200) | 110 (122) | 0.77 | 0.52 | −0.08 (0.40) | (0.57) |
| P7 | 165–500 (110–400)[d] | 260 (183) | 0.81 | 0.67 | 0.36 (0.44) | (0.54) |
| P8 | 350–420 (355–430)[d] | 382 (390) | 0.94 | 0.72 | 0.45 (0.21) | (0.43) |
| P9 | 420–510 (430–505)[d] | 461 (465) | 0.94 | 0.70 | 0.31 (0.22) | (0.44) |
| P10 | 510–700 (505–685)[d] | 593 (584) | 0.89 | 0.70 | −0.01 (0.3) | (0.46) |

[a]Correlation coefficient, mean residual, and standard deviation are all based on logarithmic values. The values in parentheses of the columns of energy range and mean energy are for GOES 7 data (GLE42-GLE52); other values are for GOES 8 and higher-numbered GOES satellites.
[b]Mean residual = $\langle x \rangle$.
[c]Standard deviation = $\langle (x - \langle x \rangle)^2 \rangle^{1/2} = (\langle x^2 \rangle - \langle x \rangle^2)^{1/2}$.
[d]GOES 7 energy range modified by *Smart and Shea* [1999], x = [log(observed) − log(predicted)].

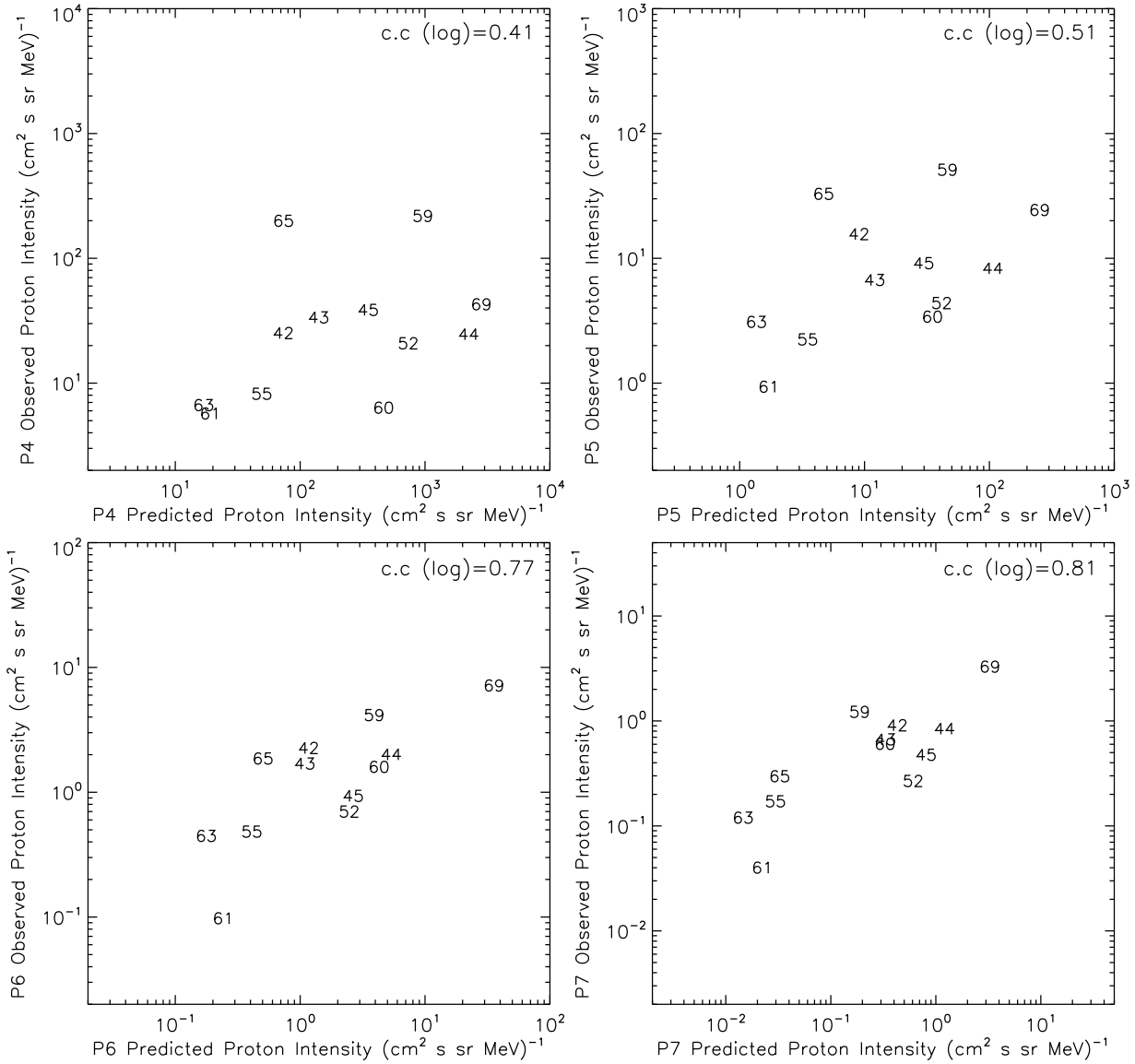


**Figure 5.** Comparison of observed GOES peak intensity with the prediction from GLE observations.

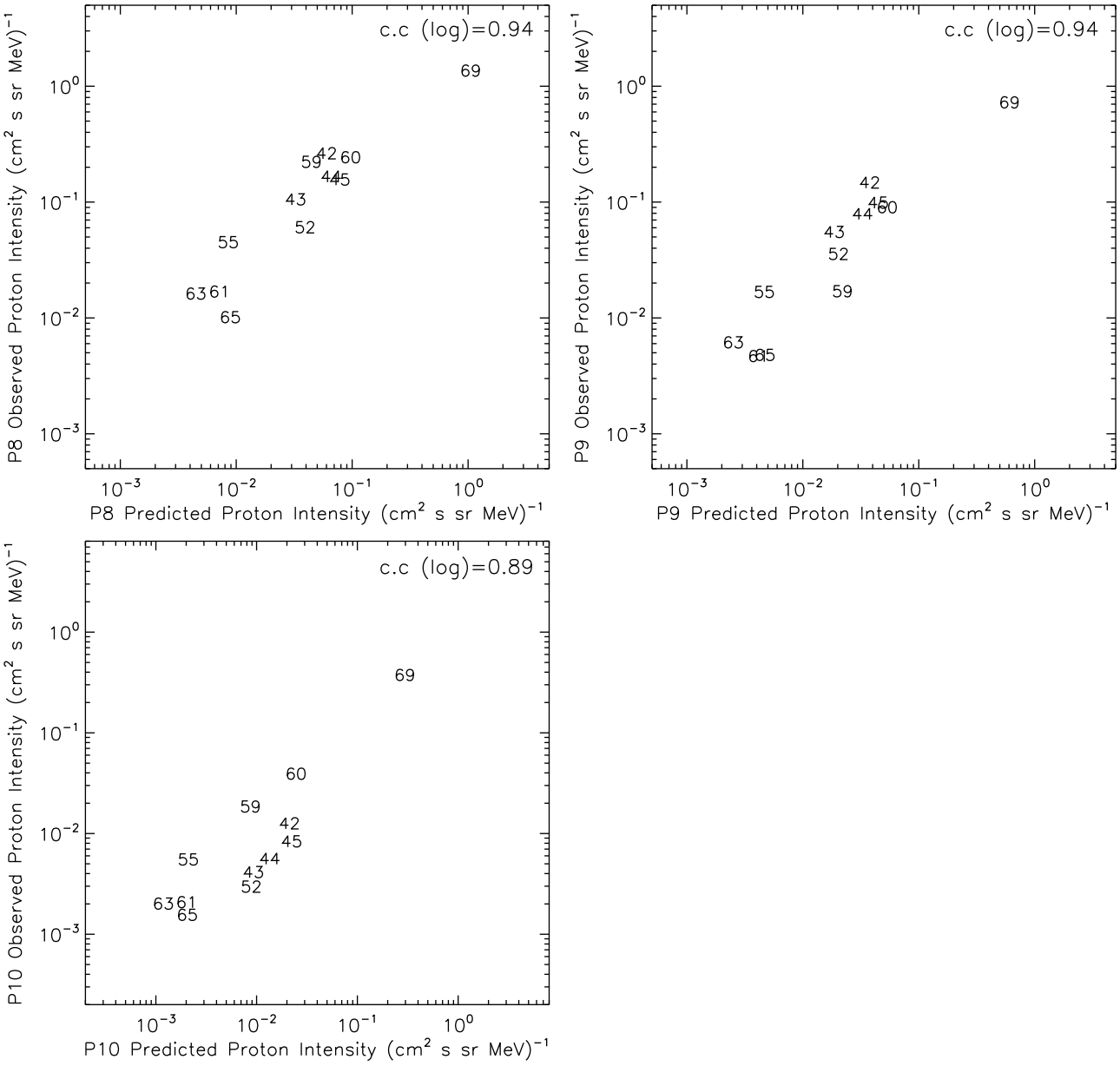


**Figure 5.** (continued)

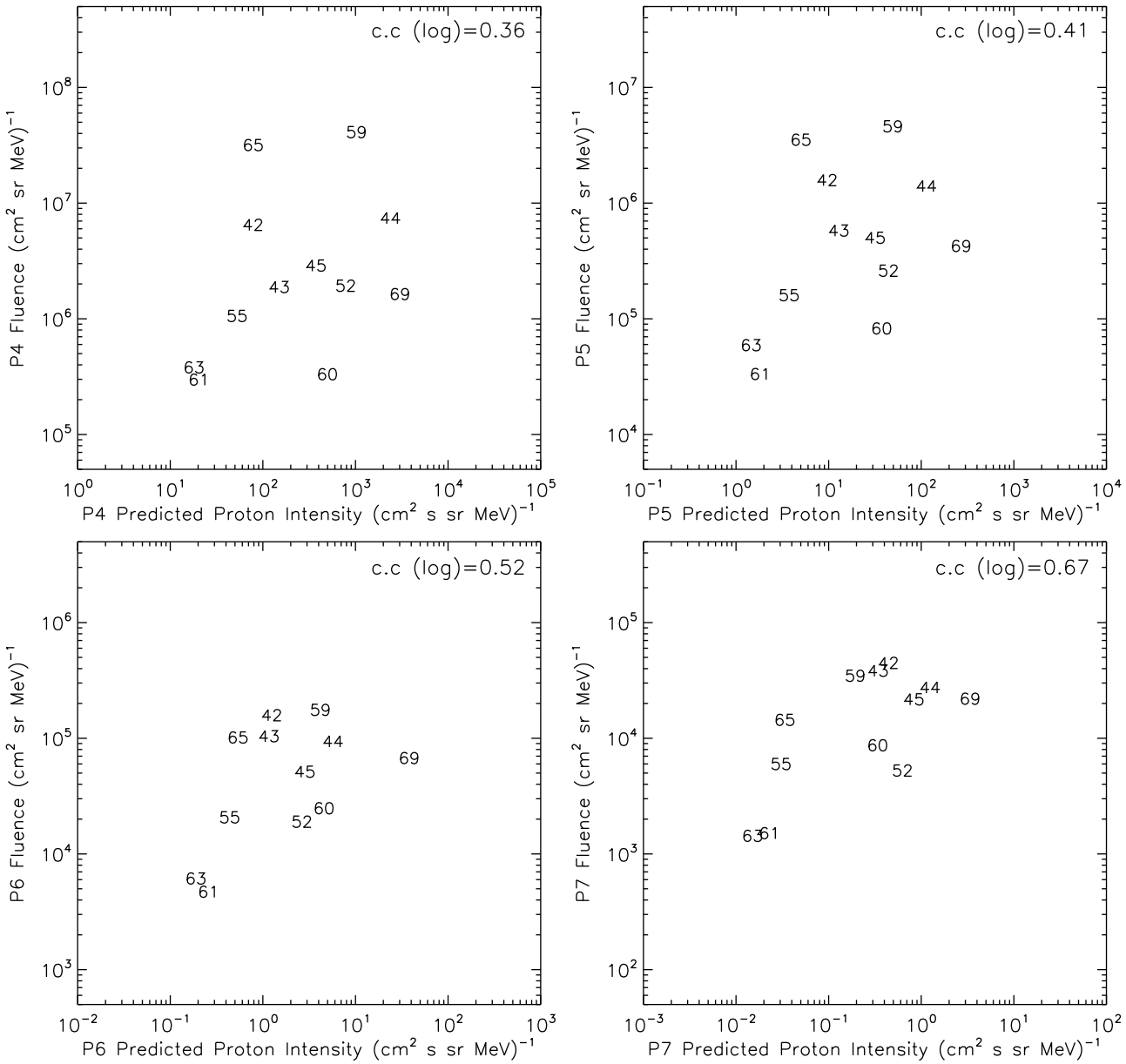


**Figure 6.** Comparison of observed GOES fluence with the peak intensity predicted from GLE observations.

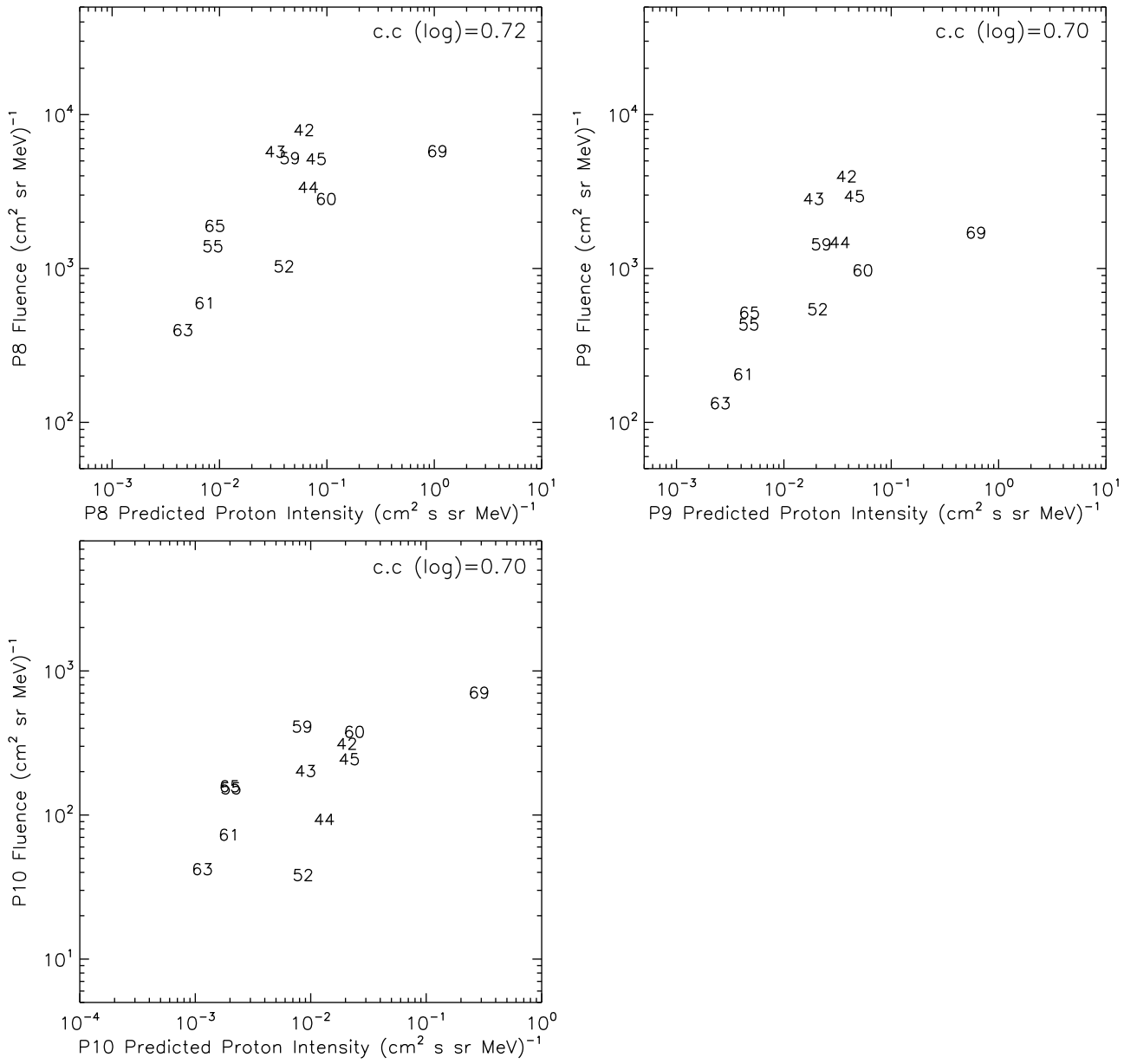


**Figure 6.** (continued)

article. We note also that a dose rate computed from peak intensity predictions would actually be a prediction of an upper limit to the peak dose rate, because different particle energies do not peak at the same time.

[23] The forecasting system is based upon measuring the energy spectrum of the relativistic component of solar cosmic rays when they peak, and then extrapolating this spectrum downward in energy to make a prediction of the peak intensity and fluence of the later-arriving particles in the tens to hundreds of MeV energy range. Because the

**Table 3.** Mean Time (in Minutes) Between Peak of GLE and Peak Flux of Each Proton Channel

| Proton Channel | Mean (Standard Deviation) | Proton Channel | Mean (Standard Deviation) |
|---|---|---|---|
| P4 | 215 (126) | P8 | 24 (17) |
| P5 | 166 (87) | P9 | 18 (17) |
| P6 | 125 (109) | P10 | 11 (17) |
| P7 | 95 (90) | | |

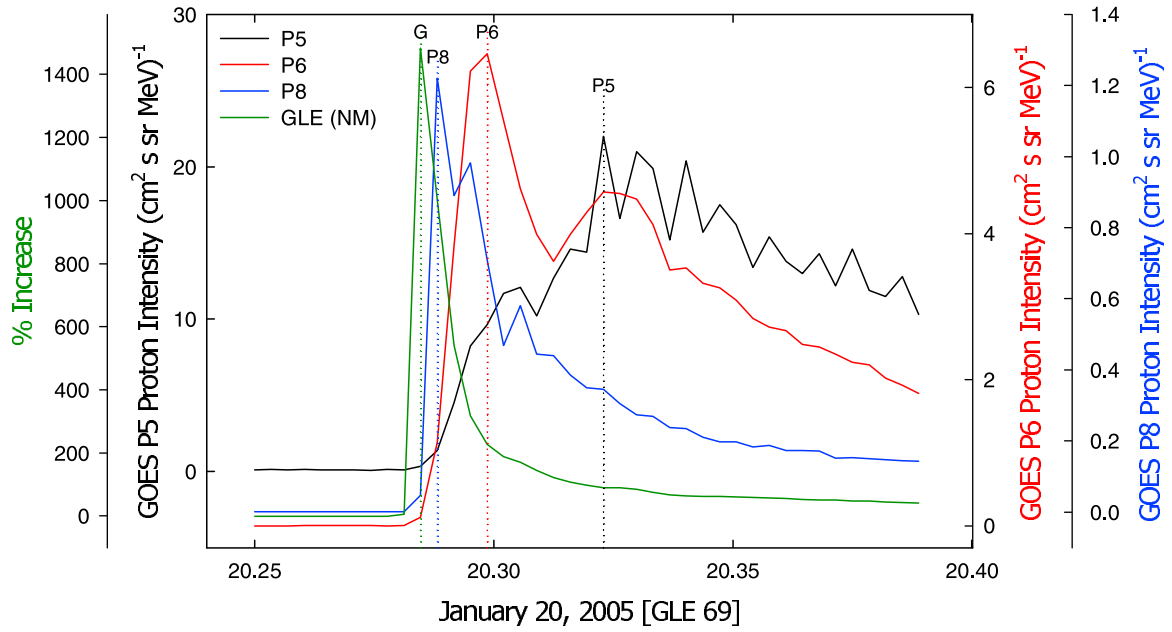


**Figure 7.** Time series for GLE 69 (20 January 2005) comparing neutron monitor count rate with fluxes from GOES proton channels P5, P6, and P8.

tens to hundreds of MeV particles are much more numerous than the GeV particles, they are of primary concern for radiation hazard to humans and electronic systems.

[24] The method employs a pair of ground-based detectors (a standard NM64 neutron monitor and a "Polar Bare" neutron monitor) with different energy responses located at Amundsen-Scott Station at the South Pole. From the different count rates of the two detectors, we derive a simple power law spectrum, which is the basis of the extrapolation to lower energy. For the lowest energy GOES channels, our method typically yields a prediction that is too high. Future improvements to this methodology might explore more complex spectral forms, such as the Band function proposed by *Tylka and Dietrich* [2009].

[25] To validate the method, we employed a database of 12 large solar particle events (ground-level enhancements, or GLE) detected by the monitors at the South Pole. The predictions (i.e., extrapolations) were compared with observations recorded in 7 differential energy channels aboard GOES spacecraft. Not surprisingly, the predictions became less accurate for lower energies, but the correlation coefficient (logarithmic) between predicted and observed was above 50% for energies down to 40 MeV in the case of peak intensity and down to 80 MeV in the case of fluence. While the correlations were weaker at lower energies, the lead times between the prediction and observation were greater, owing to velocity dispersion. For instance, the prediction of peak intensity for GOES channel P5 (40–80 MeV) occurred on average 166 min prior to the actual GOES peak. For GOES channel P7 (165–500 MeV) the corresponding lead time was 95 min.

[26] With renewed funding from NSF, an improved Polar Bare-NM64 system began operating at the South Pole in February of 2010. We are continuing development of a practical alert system for use in the coming solar maximum.

[27] **Acknowledgments.** This work was supported by the National Research Foundation of Korea with a grant funded by the South Korean Government (NRF-2009-352-C00051). This work was also supported in part by NASA grant NNX08AQ18G and by NASA/EPSCoR cooperative agreement NNX09AB05A. Resumption of South Pole observations is funded by NSF award ANT-0838839.

## References

Bieber, J. W., and P. Evenson (1991), Determination of energy spectra for the large solar particle events of 1989, *Conf. Pap. Int. Cosmic Ray Conf. 22nd*, *3*, 129–132.

Cliver, E. W., and H. V. Cane (2002), The last word: Gradual and impulsive solar energetic particle events, *Eos Trans. AGU*, *83*(7), 61, doi:10.1029/2002EO000040.

Duggal, S. P. (1979), Relativistic solar cosmic rays, *Rev. Geophys.*, *17*(5), 1021–1058, doi:10.1029/RG017i005p01021.

Feynman, J., T. P. Armstrong, L. Dao-Gibner, and S. Silverman (1990), Solar proton events during solar cycles 19, 20, and 21, *Solar Phys.*, *126*, 385–401, doi:10.1007/BF00153058.

Hu, S., M.-H. Y. Kim, G. E. McClellan, and F. A. Cucinotta (2009), Modeling the acute health effects of astronauts from exposure to large solar particle events, *Health Phys.*, *96*, 465–476, doi:10.1097/01.HP.0000339020.92837.61.

Lantos, P. (2005), Radiation doses potentially received on-board aeroplanes during recent solar particle events, *Radiat. Protec. Dosimetry*, *118*, 363–374, doi:10.1093/rpd/nci356.

Pereyaslova, N. K., M. N. Nazarova, and I. E. Petrenko (1996), An empirical statistical model of the radiation characteristics of solar proton events in near-Earth space, *Radiat. Meas.*, *26*, 451–454.

Reames, D. V. (2009), Solar release times of energetic particles in ground-level events, *Astrophys. J.*, *693*, 812–821.

Schwadron, N. A., et al. (2010), Earth-Moon-Mars radiation environment module framework, *Space Weather*, *8*, S00E02, doi:10.1029/2009SW000523.

Smart, D. F., and M. A. Shea (1999), Comment on the use of GOES solar proton data and spectra in solar proton dose calculations, *Radiat. Meas.*, *30*, 327–335.

Stoker, P. H. (1985), Spectra of solar proton ground level events using neutron monitor and neutron moderated detector recordings, *Conf. Pap. Int. Cosmic Ray Conf. 19th*, *4*, 114–117.

Tylka, A. J., and W. F. Dietrich (2009), A new and comprehensive analysis of proton spectra in ground-level enhanced (GLE) solar particle events, *Conf. Pap. Int. Cosmic Ray Conf. 31st*, *0273*, 4 pp.

Usoskin, I. G., A. J. Tylka, G. A. Kovaltsov, and W. F. Dietrich (2009), Ionization effect of strong solar particle events: Low-middle atmosphere, *Conf. Pap. Int. Cosmic Ray Conf. 31st*, *0162*, 4 pp.

Wilson, J. W., L. W. Townsend, J. E. Nealy, S. Y. Chun, B. S. Hong, W. W. Buck, S. L. Lamkin, B. D. Ganapol, F. Khan, and F. A. Cucinotta (1989), BRYNTRN: A baryon transport model, *Tech. Rep. 2887*, 84 pp., NASA, Hampton, Va.